

## Letter of Response (hess-2018-341)

We would like to thank the Editor for handling the manuscript and to thank the Referees for their insightful comments, which have helped to improve the manuscript. We provide below our detailed response to each comment (in blue). All line numbers refer to the revised marked manuscript that follows the comments and responses (insertions marked in blue and deletions in red strikethrough).

### **Referee #1**

This manuscript describes a case where water of unique quality recharges a local aquifer. The manuscript looks experimentally and through MODFLOW modeling at the expansion and mixing of the new water in the aquifer for a specific setup where recovery wells are located around the recharge pond. The concern here is desalinated water, and the main tool to distinguish these water from the background is stable isotopes.

We would like to thank the referee Prof. Alex Furman for his review and comments. We provide below our detailed response to each comment.

General comment: Sincerely, I am not sure how to treat this manuscript. On one hand addresses a question of increasing concern (globally, not only in Israel), and it describes a work properly conducted, including a very nice combination of isotopic work and a flow and transport model. On the other hand, I'm asking myself at the end of the day "what's new?" Is there something that can really be learned from this manuscript? Is it describing something that was not clear from the beginning? The innovation that I see in this paper is very specific, the use of stable isotopes to very specific types of waters. The uniqueness of the specific case is the specific O-H numbers that create very distinct end members, that possibly can lead to the ability to distinguish the mixture at very wide range of mixing ratios (this however is not explored). But mixtures of two end members, including by O-H isotopes, is not new, as the authors acknowledge. Therefore, my requirement for this paper to be accepted is to improve the description of

the unique case study throughout the manuscript, so that the innovation will be much better explained, highlighted, and discussed. If properly done this can probably be a good reference study.

Response to general comment: We emphasized the uniqueness of this work in the revised manuscript as detailed below:

1) The uniqueness of this case-study and its importance: The uniqueness of this study, as the reviewer stated, is based on the specific case where reverse-osmosis desalinated seawater (DSW) are being recharged into natural fresh groundwater (GW). There are currently only a few places that are practicing managed aquifer recharge (MAR) with DSW, but this practice will grow due to the increasing use of DSW globally. Practically all the known case studies of MAR with DSW involve brackish-water aquifers (in the Gulf countries) and not necessarily reverse-osmosis DSW. These two features are important for the contrast in heavy isotopes concentrations to be large enough to enable simple mixing calculations. (lines 56-61).

2) The novel use of isotope-transport modeling: The advantage of using stable water isotopes to trace DSW in the SAT site of the Shafdan MAR system, Israel, was recently reported by Negev et al. (2017). However, to the best of our knowledge, this is the first paper reporting groundwater modeling of reverse-osmosis desalinated seawater using isotope data. Combining a calibrated flow and transport model with isotope data enables prediction of the DSW plume spreading in the aquifer in future scenarios. This is a quantitative step ahead of previous isotope-analysis studies related to reverse-osmosis DSW in aquifers (lines 65-67).

3) The robustness of the two end-member assumption and its validation: In this work we use two features of stable water isotopes that are mutually related, in order to trace reverse-osmosis DSW in the aquifer: (1) the distinct difference between isotope composition of reverse-osmosis DSW and natural fresh water; and (2) the relative similarity of isotope composition among natural fresh water, which simplify the system to a binary mixture. See section 3.1, lines 146-147 and 160-165. The binary simplification is a robust tool for modeling DSW spreading in the aquifer, as it reduces considerably the amount of isotope data that needs to be collected and analyzed for boundary conditions. Other modeling studies that use water isotopes, implement detailed transient boundary conditions based on large data sets that vary

spatially and temporally (e.g., Reynolds and Marimuthu, 2007; Liu et al., 2014) that in most cases are not available. Mixing of two end-members is indeed widespread in geochemical studies, and can also be found in few groundwater modeling studies that use stable water isotopes as tracers (e.g., Krabbenhoft et al., 1990; Stichler et al., 2008). However, in this work an original error analysis is used to estimate the validity of the two-end-members assumption (section 3.2.3). This error analysis is possible due to the unique use of the flow and transport models discussed previously. We showed in the analysis (Fig. 6) that the assumption is valid for the current isotope-composition variability that is found in the aquifer ( $\delta^{18}\text{O}=-4.48$  to  $-5.43\%$  and  $\delta^2\text{H}=-18.41$  to  $-22.68\%$ ). We also note in the original manuscript the conditions that permit the use of a two end-members approach (lines 226-229).

Comment 1: Since the authors describe model predictions, I'm not sure if past tense is the appropriate. In the same context, instead of "results show" I'd use "results suggest".

Response 1: We agree. We revised the manuscript according to the reviewer's suggestion.

Comment 2: I do not think the model neglects fractionation (line 118). It is you (the authors) that neglect such a process. But why neglect? Is there a reason to think such a process is relevant here?

Response 2: Isotope fractionation processes such as evaporation or biogeochemical interactions are negligible during the transport of water-isotopes in deep groundwater (depth of water table  $\gg$  depth of root zone). There is strong evidence that local groundwater tends to be isotopically uniform (e.g., Krabbenhoft et al., 1990 and reference therein). Moreover, our measurements at this fast-percolating MAR site show similar isotope composition between the DSW source-water at the surface, in the variably-saturated zone and at the shallow GW (Ganot et al., 2018). Therefore, isotope fractionation even if exists in the aquifer to some extent as a slow process (centuries-millennia), it should defiantly consider negligible compared to the distinct difference between the isotope end-members. Note that the error analysis presented in section 3.2.3 (and discussed here previously) aimed to test the binary end-members

assumption, justify the assumption that isotope fractionation is negligible in this GW system. We added this explanation to the revised manuscript (in lines 125-126 and also in section 3.2.3, lines 235-240).

## **Referee #2**

As an increased using of new water resources, understanding its effect is necessary. The desalinated seawater is a potential water resource with the increasing demands of fresh water all around the world in the modern days. This manuscript introduces a new insight of stable isotope application in water research. An isotopic solute transport model was built to estimate the spread of the desalinated seawater in the coastal aquifer. It is not common to see applying the stable isotope method by a numerical model, considering the wide range of isotopes of the water bodies. Authors take the advantage of the conservation isotope concentration of the DSW, so that they can simplify the local water sources to groundwater into a binary system in the sight of isotopic concentration. To be honest, this manuscript is very interesting but it is really hard for me to make a comment on it. Generally, it is a useful and convincing study, but it lacks novelty on method. So my suggestion is accepted after revision.

We are very contented that referee #2 summarized the significance of this work in its two most unique features. The extreme difference in the isotopic signature between reverse-osmosis DSW and all other sources of natural fresh water that makes the binary system approximation solid, and the data-based flow and transport model of water isotopes and its simulations. The novelty of this study was discussed in our response to the general comment of referee #1.

General comment: The number and type of water samples are not clear in this manuscript. Since the rainwater and the runoff water in the setting pond are regarded as water sources to the groundwater, it should be more specific of the isotope data, especially, the runoff water.

Response to General comment: We added a detailed description of the water samples to the revised manuscript, including water sample type and number of samples (lines 86-88 and Table S1 in the Supplement). Please see more details in the following responses to the specific comments.

Comment 1: How many isotopic water samples do you have?

Response 1: We have a total of 61 isotope samples, where each sample was analyzed for  $^{18}\text{O}$  and  $^2\text{H}$  isotopes. 42 samples were sampled from groundwater production wells. The remaining samples were sampled from several sources: (1) the DSW inlet pipe, (2) few locations inside the DSW infiltration pond, (3) runoff canal, and (4) shallow observation wells (OA and OB). We added this information to the revised manuscript (lines 86-88 and Table S1 in the Supplement).

Comment 2: Is there any water samples of rain or runoff water in the ponds? Line 124

Response 2: We did not sample rainwater in this study and instead we used the rain-water data from Gat and Dansgaard (1972) as described in lines 162-163. We have water samples from one runoff event ( $\delta^{18}\text{O}=-4.77\text{‰}$  and  $\delta^2\text{H}=-19.5\text{‰}$ ) that was taken on January 2017 (very similar to the rain composition of  $\delta^2\text{H}=-19.9\text{‰}$  line 162). Unfortunately, we have no samples from the runoff event of 2015 (line 142-143) and we assumed the runoff isotope composition of 2015 is similar to 2017. This information added to the revised manuscript (lines 86-88 and Table S1 in the Supplement).

Comment 3: How did you deal with these values? The lowest and highest? For example, the lowest  $C_{\text{GW}}$   $\delta^{18}\text{O}=-5.43\text{‰}$   $\delta^2\text{H}=-22.68\text{‰}$  is this the result of one sample or the lowest values of all groundwater samples? Why? Line 121.

Response 3: We normalized the concentrations to the lowest value that was measured in the aquifer (i.e., based on one sample). Next, in section 3.2.3 (line 215) we check this assumption by normalizing the concentrations to the highest value (also based on one sample) and then compare the simulation results of these two extreme options (Fig. 6). We show that the results are almost similar (less than 1% difference) in the aquifer area next to the infiltration ponds. Hence, in similar isotope binary systems, a

practical conclusion of this analysis will be to use an average isotope value to normalize the isotope concentrations in the aquifer. We added this explanation to the revised manuscript (lines 229-232)

Comment 4: Is there any soluble salt in the study area? Line 150

Response 4: There is no extensive soluble salt layer/formation according to the recent available geological data. In Ganot et al., 2018 (Table 1) it is shown that chloride concentrations are similar in: (1) pond water of the infiltration basin; (2) variably saturated zone (suction cups at 0.5-3 m below surface); and (3) shallow groundwater below the pond. Therefore, dissolution of chloride during infiltration is negligible. Chloride concentration of naturally infiltrating groundwater is mostly related to evapotranspiration which concentrates the rainwater with respect to the conservative chloride ion. Nevertheless, the binary system approach used in this study based on conservative water-isotope tracers is superior to both conservative and nonconservative classic tracers. This is an important insight - thank you. We added this information to the revised manuscript (lines 155-156 and 163-165).

Comment 5: Do you have any data from modern rainwater? Is that too old for your study? 1972? Line 153

Response 5: The paper of Gat and Dansgaard (1972) is the most comprehensive survey published on stable isotopes of fresh water in Israel. It includes rain samples that were collected next to the Menashe MAR site and were used in this study. A more recent study (Goldsmith et al., 2017) reports similar values ( $\delta^{18}\text{O} = -5.1\text{‰}$  to  $-5.7\text{‰}$ ;  $\delta^2\text{H} = -18.6\text{‰}$  to  $-25.6\text{‰}$ ) for rain samples collected at the coastal plain of Israel, but it based on fewer sampling station and with no sampling point next to Menashe MAR site. We added this reference to the manuscript (line 163).

Comment 6: All the advantages listed in the manuscript of using the method show that it is specific lucky for this area. Can you give some descriptions to show the universal applicability?

Response 6: The advantage of using stable water isotopes for tracing reverse-osmosis desalinated water in various downstream water systems is already known from previous studies (Ganot et al., 2018; Kloppmann et al., 2008a, 2008b; Kloppmann et al., 2018; Negev et al., 2017). In this study we use this advantage in a modeling framework to predict future mixing and spreading trends of DSW in the aquifer. Therefore, the modeling approach presented in this study can be used in other sites (e.g., Mazariegos et al., 2017; Negev et al., 2017; Stuyfzand et al., 2017) to predict reverse-osmosis desalinated-water distribution in aquifers. As the production of DSW using reverse-osmosis is projected to increase (Hanasaki et al., 2016) and the use of MAR system widens (e.g., Rodríguez-Escales et al., 2018) we are sure that the advantage listed in this manuscript is/will be highly relevant for more MAR hydrologists. Above seawater desalination and MAR, integrating water resources is a key for dealing with increasing water demands and droughts, hence operations of similar features are expected to develop first in semi-arid regions but also in more temperate climates. We added these arguments to the revised manuscript (lines 56-61 and 272-277).

## References

- Ganot, Y., Holtzman, R., Weisbrod, N., Russak, A., Katz, Y. and Kurtzman, D.: Geochemical Processes During Managed Aquifer Recharge With Desalinated Seawater, *Water Resources Research*, 54(2), 978–994, doi:10.1002/2017WR021798, 2018.
- Gat, J. R. and Dansgaard, W.: Stable isotope survey of the fresh water occurrences in Israel and the Northern Jordan Rift Valley, *Journal of Hydrology*, 16(3), 177–211, doi:10.1016/0022-1694(72)90052-2, 1972.
- Goldsmith, Y., Polissar, P. J., Ayalon, A., Bar-Matthews, M., deMenocal, P. B. and Broecker, W. S.: The modern and Last Glacial Maximum hydrological cycles of the Eastern Mediterranean and the Levant from a water isotope perspective, *Earth and Planetary Science Letters*, 457, 302–312, doi:10.1016/j.epsl.2016.10.017, 2017.
- Kloppmann, W., Vengosh, A., Guerrot, C., Millot, R. and Pankratov, I.: Isotope and Ion Selectivity in Reverse Osmosis Desalination: Geochemical Tracers for Man-made Freshwater, *Environmental Science & Technology*, 42(13), 4723–4731, doi:10.1021/es7028894, 2008a.
- Kloppmann, W., Van Houtte, E., Picot, G., Vandenbohede, A., Lebbe, L., Guerrot, C., Millot, R., Gaus, I. and Wintgens, T.: Monitoring Reverse Osmosis Treated Wastewater Recharge into a Coastal Aquifer by Environmental Isotopes (B, Li, O, H), *Environmental Science & Technology*, 42(23), 8759–8765, doi:10.1021/es8011222, 2008b.

Krabbenhoft, D. P., Anderson, M. P. and Bowser, C. J.: Estimating groundwater exchange with lakes: 2. Calibration of a three-dimensional, solute transport model to a stable isotope plume, *Water Resour. Res.*, 26(10), 2455–2462, doi:10.1029/WR026i010p02455, 1990.

Liu, Y., Yamanaka, T., Zhou, X., Tian, F. and Ma, W.: Combined use of tracer approach and numerical simulation to estimate groundwater recharge in an alluvial aquifer system: A case study of Nasunogahara area, central Japan, *Journal of Hydrology*, 519, 833–847, doi:10.1016/j.jhydrol.2014.08.017, 2014.

Mazariegos, J. G., Walker, J. C., Xu, X. and Czimczik, C. I.: Tracing Artificially Recharged Groundwater using Water and Carbon Isotopes, *Radiocarb. Tucson*, 59(2), 407–421, doi:http://dx.doi.org/10.1017/RDC.2016.51, 2017.

Negev, I., Guttman, J. and Kloppmann, W.: The Use of Stable Water Isotopes as Tracers in Soil Aquifer Treatment (SAT) and in Regional Water Systems, *Water*, 9(2), 73, doi:10.3390/w9020073, 2017.

Reynolds, D. A. and Marimuthu, S.: Deuterium composition and flow path analysis as additional calibration targets to calibrate groundwater flow simulation in a coastal wetlands system, *Hydrogeol J*, 15(3), 515–535, doi:10.1007/s10040-006-0113-5, 2007.

Stichler, W., Maloszewski, P., Bertleff, B. and Watzel, R.: Use of environmental isotopes to define the capture zone of a drinking water supply situated near a dredge lake, *Journal of Hydrology*, 362(3), 220–233, doi:10.1016/j.jhydrol.2008.08.024, 2008.

# Managed aquifer recharge with reverse-osmosis desalinated seawater: modeling the spreading in groundwater using stable water isotopes

Yonatan Ganot<sup>1,2,a</sup>, Ran Holtzman<sup>2</sup>, Noam Weisbrod<sup>3</sup>, Anat Bernstein<sup>3</sup>, Hagar Siebner<sup>3</sup>, Yoram Katz<sup>4</sup>, and Daniel Kurtzman<sup>1</sup>

<sup>1</sup>Institute of Soil, Water and Environmental Sciences, The Volcani Center, Agricultural Research Organization, Rishon LeZion, 7505101, Israel

<sup>2</sup>Department of Soil and Water Sciences, The Hebrew University of Jerusalem, Rehovot, 7610001, Israel

<sup>3</sup>Department of Environmental Hydrology & Microbiology, Zuckerberg Institute for Water Research, Jacob Blaustein Institutes for Desert Research, Ben-Gurion University of the Negev, Midreshet Ben-Gurion, 8499000, Israel

<sup>4</sup>Mekorot, Water Company Ltd, Tel Aviv, 6713402, Israel

<sup>a</sup>now at: Department of Land, Air, and Water Resources, University of California, Davis, 95616, USA

Correspondence to: Yonatan Ganot ([yonatan.ganot@mail.huji.ac.il](mailto:yonatan.ganot@mail.huji.ac.il))

**Abstract.** The spreading of reverse-osmosis desalinated seawater (DSW) in the Israeli Coastal Aquifer was studied using groundwater modeling and stable water isotopes as tracers. The DSW produced at the Hadera seawater reverse osmosis (SWRO) desalination plant is recharged into the aquifer through infiltration pond at the managed aquifer recharge (MAR) site of Menashe, Israel. The distinct difference in isotope composition between DSW ( $\delta^{18}\text{O}=1.41$ ;  $\delta^2\text{H}=11.34\text{‰}$ ) and the natural groundwater ( $\delta^{18}\text{O}=-4.48$  to  $-5.43\text{‰}$ ;  $\delta^2\text{H}=-18.41$  to  $-22.68\text{‰}$ ) makes the water isotopes a preferable tracer compared to widely-used chemical tracers, such as chloride. Moreover, this distinct difference can be used to simplify the system to a binary mixture of two end members: desalinated seawater and groundwater. This approach is validated through a sensitivity analysis and it is especially robust when spatial data of stable water isotopes in the aquifer is scarce. A calibrated groundwater flow and transport model was used to predict the DSW plume distribution in the aquifer after 50 years of MAR with DSW. The results show-suggest that after 50 years 94% of the recharged DSW was recovered by the production wells at the Menashe MAR site. The presented methodology is useful for predicting the distribution of reverse-osmosis desalinated seawater in various downstream groundwater systems.

## 1 Introduction

Desalinated seawater global production is projected to double by 2040 while extending its geographical extent (Hanasaki et al., 2016). In some regions, desalinated seawater (DSW) is already the main source for fresh water (Dawoud, 2005). In Israel, for example, DSW reached ~~80~~66% of the domestic and industrial fresh water supply in 2017 (Israel Water Authority, ~~2017~~2018). This growing use of DSW affects downstream water systems such as reservoirs (Ronen-Eliraz et al., 2017; Negev et al., 2017; Stuyfzand et al., 2017; Ganot et al., 2017, 2018), wastewater treatment plants (Lahav et al., 2010; Negev et al.,

32 2017) and agricultural irrigation (Lahav et al., 2010; Yermiyahu et al., 2007). One direct way by which DSW use affects the  
33 water budget is Managed Aquifer Recharge (MAR). MAR using different water sources has been practiced for over 5 decades  
34 as part of the integrated water resource management of Israel (Dreizin et al., 2008; Gvirtzman, 2002), and is becoming a major  
35 component of water management in many Mediterranean countries (Rodríguez-Escales et al., 2018). Excess DSW produced  
36 in Israel due to operational constraints made it an attractive alternative source for MAR, raising the need to understand its  
37 effect. While the relatively rapid hydrological and geochemical processes (timescales of hours to weeks) of this new MAR  
38 activity were recently monitored and modeled (Ganot et al., 2017, 2018; Ronen-Eliraz et al., 2017), the potential long-term  
39 (months to decades) impact of this process on the natural aquifer is yet unknown, lacking observations and quantitative studies.  
40 Stable water isotopes  $^{18}\text{O}$  and  $^2\text{H}$  are excellent tracers for water generated by seawater reverse osmosis (SWRO) desalination.  
41 The lack of fractionation during the reverse-osmosis process, in contrast with various isotope-fractionation processes occurring  
42 in natural fresh water (Al-Basheer et al., 2017; Gat, 1996; Kloppmann et al., 2008a, 2008b), is the cause of the distinct  
43 difference in isotope composition between reverse-osmosis DSW and groundwater (GW) originating from natural fresh water  
44 (Ganot et al., 2018; Kloppmann et al., 2018; Negev et al., 2017). For example, the advantage of using  $^{18}\text{O}$  and  $^2\text{H}$  as a  
45 quantitative tool for tracing [treated wastewater \(originated from DSW\)](#) mixing with GW was recently demonstrated by  
46 comparing the mixing ratios of chloride, carbamazepine and water isotopes in the soil-aquifer-treatment (SAT) site at the  
47 Shafdan MAR system, Israel (Negev et al., 2017).

48 Here, we use stable water isotope to trace spreading of DSW in the aquifer and the production wells within the MAR site of  
49 Menashe, Israel. The DSW is produced at the Hadera SWRO desalination plant, which operates since 2010 with an annual  
50 production capacity of 130 million cubic meters (MCM). It is one of five large SWRO desalination plants (production capacity  
51  $\geq 90$  MCM, per year per plant) that were built along the Mediterranean coast of Israel during 2005–2015 (Stanhill et al., 2015).  
52 The DSW is regularly supplied directly to consumers through the centralized national water system. Periodically, operational  
53 constraints such as maintenance of the national system prohibit distribution of the DSW; limited reservoir capacity makes  
54 storage of this expensive surplus of DSW in the aquifer through MAR operations the only feasible solution (Ganot et al., 2017,  
55 2018; Ronen-Eliraz et al., 2017).

56 [There are currently only a few places that are practicing MAR with DSW, but this practice is expected to grow due to the](#)  
57 [increasing use of DSW globally. Practically, most of the known case studies of MAR with DSW involve brackish-water](#)  
58 [aquifers \(mainly in the Gulf countries\) and not necessarily reverse-osmosis DSW. In this work we present a unique case-study](#)  
59 [that explores the spreading of reverse-osmosis DSW plume in a fresh-water aquifer. The use of two isotope-distinguish end-](#)  
60 [members, in this case, reverse-osmosis DSW and natural fresh GW, are prerequisite to implement the analysis presented in](#)  
61 [this paper.](#)

62 Predicting the long-term DSW distribution in the aquifer and the production wells is the main objective of this study. We  
63 incorporate water isotope data of  $^{18}\text{O}$  and  $^2\text{H}$  in a regional GW flow and transport model (e.g., Boronina et al., 2005;  
64 Krabbenhoft et al., 1990; Liu et al., 2014; Reynolds and Marimuthu, 2007; Stichler et al., 2008) in order to predict DSW  
65 distribution in the aquifer. While the methodology for measuring the present mixing of DSW and GW was reported previously

66 (Negev et al., 2017), in the current study our GW modeling approach allows us to predict future mixing trends in the production  
67 wells of the Menashe MAR site. Predicting DSW distribution in the aquifer is of main interest from water quantity (estimating  
68 the recovery potential of DSW originate from MAR) and quality perspectives (e.g., Birmhack et al., 2011; Ganot et al., 2018  
69 and references therein).

## 70 **2 Methods**

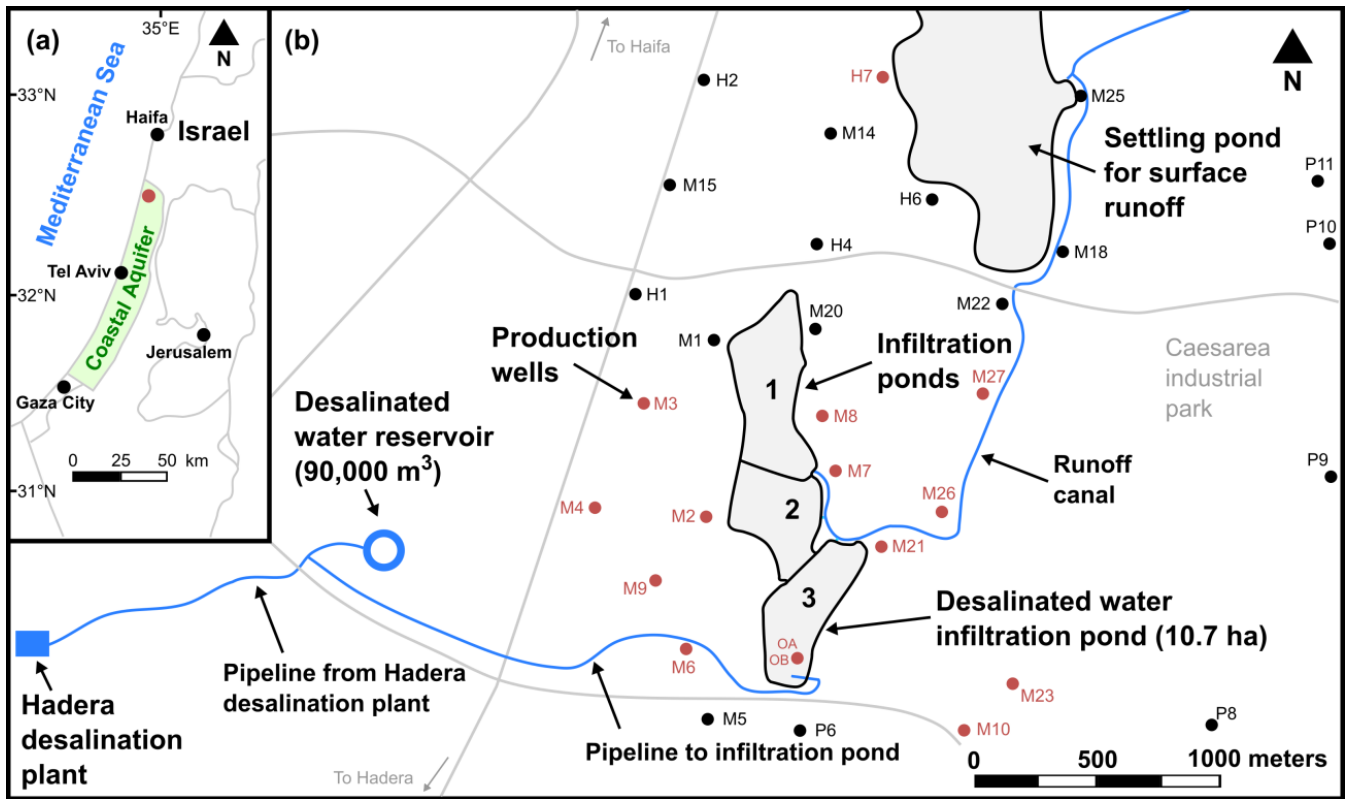
### 71 **2.1 Study area**

72 The Menashe MAR site is located on sand dunes 28 m above sea level, in the northern part of the Israeli Coastal Aquifer, an  
73 unconfined sandy aquifer stretching over an area of 2000 km<sup>2</sup> along the Mediterranean coast (Fig. 1a). The local climate is  
74 Mediterranean, with an annual average temperature of 20.2°C, and annual mean precipitation of 566 mm yr<sup>-1</sup> (Israel  
75 Meteorological Service, 2014). The aquifer thickness varies from 100 m on the coastline (to the west of the Menashe site) to  
76 few meters in the east. It is composed of Pleistocene calcareous sandstone interleaved with discontinuous marine and  
77 continental silt, and clay lenses. Thick Neogene clay (Saqiye Group), which is highly impermeable, underlies the aquifer  
78 (Kurtzman et al., 2012). Regional groundwater level is ~3 m above mean sea level (September 2014, Israel Water Authority,  
79 2014) and the characteristic aquifer properties are: hydraulic conductivity of 10 m d<sup>-1</sup>, storativity of 0.25 and porosity of 0.4  
80 (Shavit and Furman, 2001).

81 The Menashe MAR site diverts the natural ephemeral flows from the Menashe-Hills streams into a settling pond and from  
82 there to three infiltration ponds. Production wells that encircle the site recover the recharged water from the aquifer (Sellinger  
83 and Aberbach, 1973). In the last few years, the southern infiltration-pond is dedicated for infiltration of surplus of DSW from  
84 the Hadera SWRO desalination plant, located 4 km to the west, on the coastline (Fig. 1b).

### 85 **2.2 Water sampling**

86 Groundwater from 14 wells at the Menashe MAR site were sampled biannually during 2015 to 2017 (n=42). In addition, ~~DSW~~  
87 ~~water was were~~ sampled from the infiltration pond DSW inlet pipe (n=3), ~~few locations inside the pond during MAR events~~  
88 ~~(n=4), shallow observation wells (OA and OB; n=11) and runoff canal (n=1) during MAR events.~~ Stable water isotopes  
89 (expressed as  $\delta^{18}\text{O}$  and  $\delta^2\text{H}$  in ‰ vs. the VSMOW – Vienna Standard Mean Ocean Water) were measured by Cavity Ring-  
90 Down Spectroscopy (CRDS) analyzer (L2130-i, Picarro).



91

92

93

94

**Figure 1. Map of the study area. (a) Location of the Israeli Coastal Aquifer and the Menashe MAR site (red circle). (b) The Menashe MAR site. Surplus of desalinated seawater is delivered from Hadera SWRO desalination plant (lower left) to the southern infiltration basin (pond 3). The red dots represent wells that were sampled for water isotope analysis.**

95

### 2.3 Groundwater flow and transport model

96

97

98

99

100

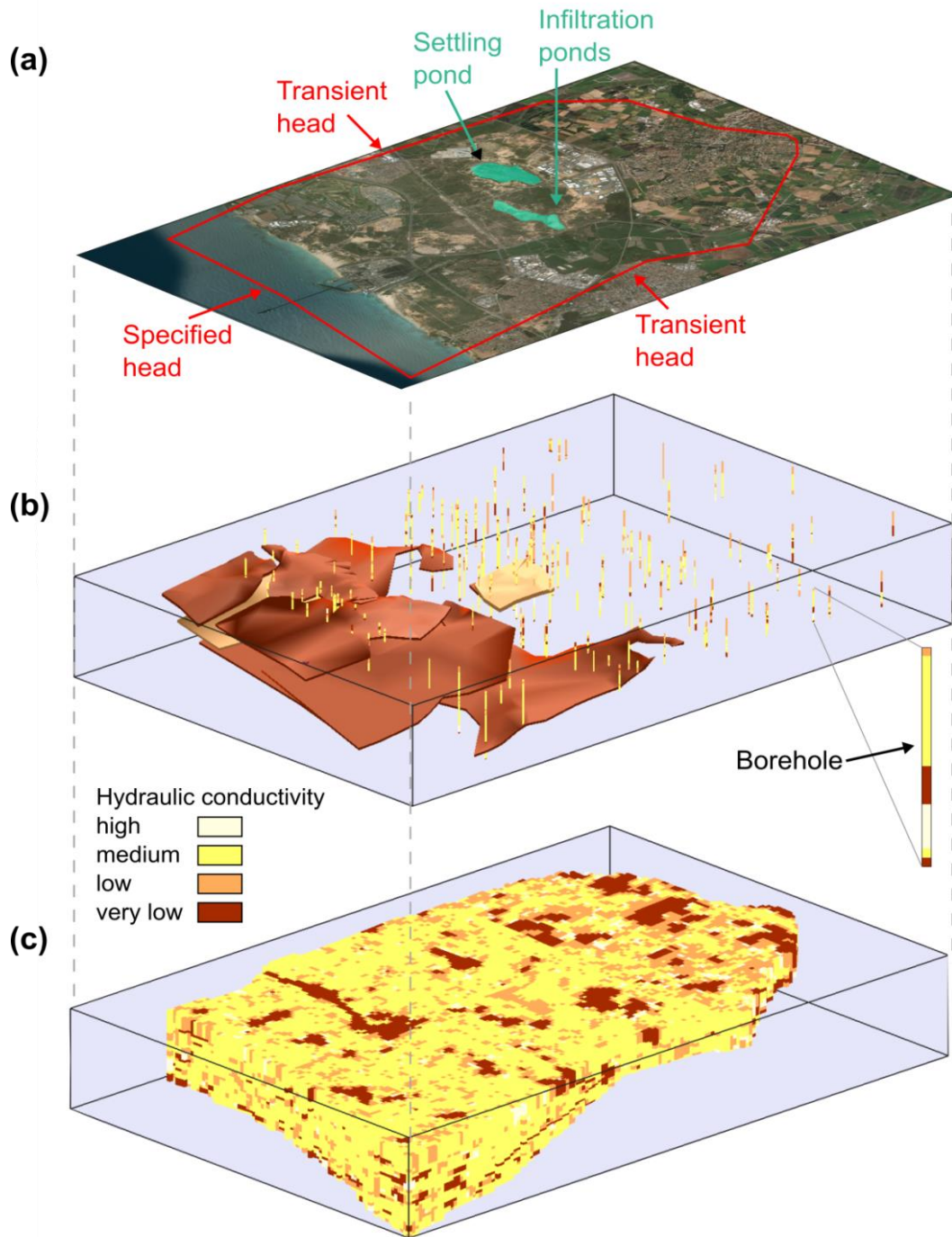
101

102

103

104

A detailed three-dimensional transient water flow and solute transport model was set up in order to estimate DSW spreading in the aquifer at the Menashe site area. The model covers an area of 65 km<sup>2</sup> including a western out-shore strip of 9 km<sup>2</sup> (Fig. 2a). The geological data processed from well logs, geological and structural maps served as the basis for the conceptual model, constructed via the GMS software package (version 10.3; www.aquaveo.com). The variety of rock types was grouped into four hydro-geological units, each characterized by a set of hydrological properties (Table 1). Over 100 well logs were analyzed using the T-PROGS software (Carle, 1999) and provided the spatial distribution of the hydro-geological units. This geostatistically generated unit array, conditioned to the boreholes logs, was combined with structural map data of the major marine clay lenses present in the aquifer. The resulting model hence reflects the hydro-geological units' proportions and transition trends as well as the division into sub aquifers by marine clay within the western part of the aquifer (Fig. 2b, c).



105

106

107

108

**Figure 2.** The model used in simulations of water flow and solute transport. (a) The modeled area and boundary conditions. (b) The major continuous marine clay lenses, and the boreholes log. (c) The combined deterministic and geostatistically-generated material array representing the aquifer in the model.

109 **Table 1. Major rock types in the study area grouped into four hydro-geological units**

Hydro-geological unit	1	2	3	4
<b>Rock types</b>	Gravel, beach rock, Kurkar with shells/gravel	Calcareous sandstone (Kurkar), sand	Loam, sandy loam, loamy sand, marine silty sand	Clay/silt of marine or terrestrial origin
<b>Hydraulic conductivity (K)</b>	High	Medium	Low	Very low
<b>Unit proportions (%)</b>	4	59	23.5	13.5

110

111 The model domain was discretized horizontally into 70 X 70 m mesh cells. The vertical section of the aquifer, of thickness  
 112 ranging 50–100 m from east to west, was divided into 24 layers with vertical spatial-resolution of 5 m or smaller. The model  
 113 bottom boundary was defined by the impermeable Saqiye Group underlying the aquifer. The model top boundary was defined  
 114 by the water table representing an unconfined aquifer. Boundary conditions along the northern, eastern and southern model  
 115 boundaries were set to be of transient head, based on periodical water level measurements. The western boundary was set to a  
 116 constant head boundary dictated by the sea level. Initial conditions were based on static heads measured at several dozens of  
 117 production and observation wells included in the model. Sources and sinks in the flow model include recharge by precipitation,  
 118 MAR (both runoff and DSW recharge) and production wells. Natural recharge from precipitation was based on adjacent rain  
 119 gauge measurements (Gan Shemuel) using an average recharge coefficient of 0.4 (which is representative of sands). Recharge  
 120 flux of DSW by MAR activity was calculated by a variably-saturated model of the upper 30 m of the sediment under the  
 121 southern infiltration pond (Ganot et al., 2017). Pumping activity of the production wells was based on a database from the  
 122 national water company of Israel, Mekorot.

123 The transport model considers the stable water isotopes  $^{18}\text{O}$  and  $^2\text{H}$  as conservative tracers, i.e. neglecting isotope fractionation  
 124 (there is strong evidence that local groundwater tends to be isotopically uniform, see for example Krabbenhoft et al., 1990 and  
 125 reference therein). We normalize the tracer concentration as  $C = (\delta - \delta_{\min}) / (\delta_{\max} - \delta_{\min})$ , where  $\delta$  is the isotope composition of  
 126  $\delta^{18}\text{O}$  or  $\delta^2\text{H}$  in the aquifer, and  $\delta_{\min}$  and  $\delta_{\max}$  the minimum and maximum isotope composition. Since practically  $\delta_{\max} = \delta_{\text{DSW}}$ ,  
 127 the normalized concentration of DSW is  $C_{\text{DSW}} = 1$ , whereas that of GW ranges from  $C_{\text{GW}} = 0$  ( $\delta^{18}\text{O} = -5.43\%$ ,  $\delta^2\text{H} = -22.68\%$ ) to  
 128  $C_{\text{GW}} = 0.13$  ( $\delta^{18}\text{O} = -4.48\%$ ,  $\delta^2\text{H} = -18.41\%$ ). Boundary conditions of the transport model are of specified mass flux ( $=qC$ , where  
 129  $q$  is the specific discharge), with zero flux at the bottom boundary (considered impermeable), as well as zero flux at the  
 130 northern, eastern and southern boundaries, and also with the precipitation and the runoff-ponds source terms due to their GW  
 131 isotopes composition ( $C_{\text{GW}} = 0$ ). Mass flux with DSW isotopes composition ( $C_{\text{DSW}} = 1$ ) is given at the western boundary (sea)  
 132 and the DSW infiltration pond source term. The validity of the use of a single value ( $C_{\text{GW}} = 0$ ) for the GW mass-flux boundaries,  
 133 in light of the range of isotope composition in the aquifer prior to MAR of DSW ( $\delta^{18}\text{O} = -4.48$  to  $-5.43\%$  and  $\delta^2\text{H} = -18.41$  to  $-$   
 134  $22.68\%$ ), is discussed in Section 3.2.3. Initial conditions were set by interpolating the water isotope data from several  
 135 production wells.

136 The MODFLOW (Harbaugh et al., 2000) and MT3DMS (Zheng and Wang, 1999) codes were used through the GMS user  
 137 interface to solve numerically the flow and transport models, respectively. Both codes, which use finite difference scheme, are

138 considered reliable and are therefore widely used for regional aquifer modeling (Zhou and Li, 2011). The flow and transport  
139 model was calibrated using a dataset from 2015 to 2017. During 2015, 2016 and 2017 a volume of 2.6, 1.3 and 0.6 MCM of  
140 DSW were recharged, respectively, at the MAR Menashe site. In these years the MAR events were non-continuous discharge  
141 of DSW to pond 3 (Fig. 1b) during January and/or February (Ganot et al., 2017, 2018). In addition, a volume of 3.2 and 1.6  
142 MCM of runoff water were discharged to the settling pond during 2015 and 2017, respectively.

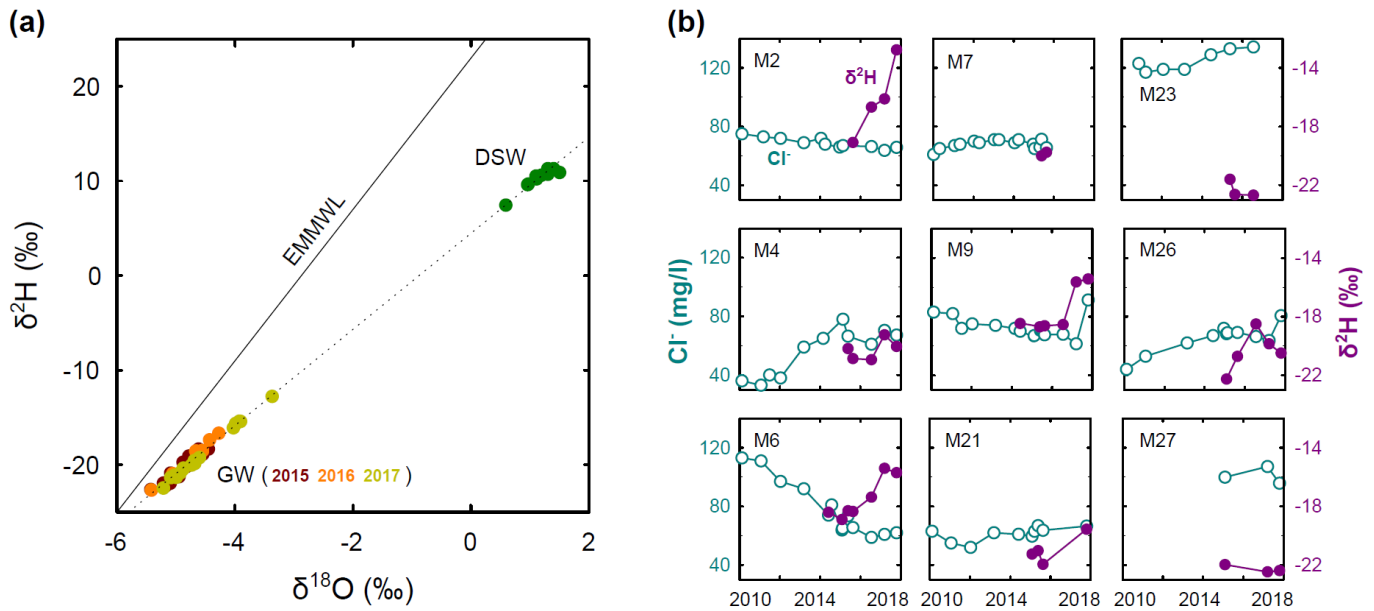
### 143 **3. Results and discussion**

#### 144 **3.1 Water isotopes**

145 The distinct difference between the water isotopes of the production wells and DSW is shown in a  $\delta^2\text{H}$  vs.  $\delta^{18}\text{O}$  diagram for  
146 the period of 2015 to 2017 (Fig. 3a and Table S1 in the Supplement). During 2016 and more prominently in 2017, few wells  
147 show a progressive change in composition towards higher isotope values—a transition from GW towards DSW on the mixing  
148 line (Fig. 3a), which indicates mixing with DSW, while most wells retain constant isotope composition. Note that for all  
149 samples in Fig. 3a there is a strong linear correlation between  $\delta^{18}\text{O}$  and  $\delta^2\text{H}$  ( $R^2=0.9991$ ); thus, hereafter we only report  $\delta^2\text{H}$  as  
150 a tracer.

151 The isotope composition of  $\delta^2\text{H}$  and the concentration of chloride are shown for comparison in nine wells during the years  
152 2010 to 2018 (Fig. 3b). The chloride concentration of DSW at the Menashe MAR site is always lower than 10 mg/l (Ganot et  
153 al., 2018), while in the local GW it is found in a wider range of 40 to 140 mg/l. The large chloride concentration variability in  
154 the different wells prior to MAR with DSW (before 2015) suggests that various water sources feed the aquifer (as there is no  
155 extensive soluble salt layer in the aquifer according to the recent available geological data). Moreover, the breakthrough of  
156 DSW in wells M2, M6 and M9 captured by an increase in  $\delta^2\text{H}$  is not reflected in the chloride concentration (expected to  
157 decrease). This implies that chloride—in general a widely used conservative tracer, is less sensitive to reverse-osmosis DSW  
158 in natural fresh GW systems and therefore less useful for its detection.

159 Finally, we note that the very different DSW signature in terms of  $\delta^2\text{H}$  from the other water sources in the Menashe site,  
160 reduces the problem of mixing various water sources to a binary system: (i) DSW and (ii) all other natural sources. This is  
161 because the signatures of runoff water ( $\delta^{18}\text{O}=-4.77\text{‰}$  and  $\delta^2\text{H}=-19.5\text{‰}$ ) and rainwater ( $\delta^{18}\text{O}=-5.8\text{‰}$  and  $\delta^2\text{H}=-19.9\text{‰}$ ; Gat  
162 and Dansgaard, 1972; Goldsmith et al., 2017) are very similar to that of the local GW. Therefore, the binary system approach  
163 used in this study, which is based on conservative water-isotope tracers is superior to both conservative and nonconservative  
164 chemical tracers.



165

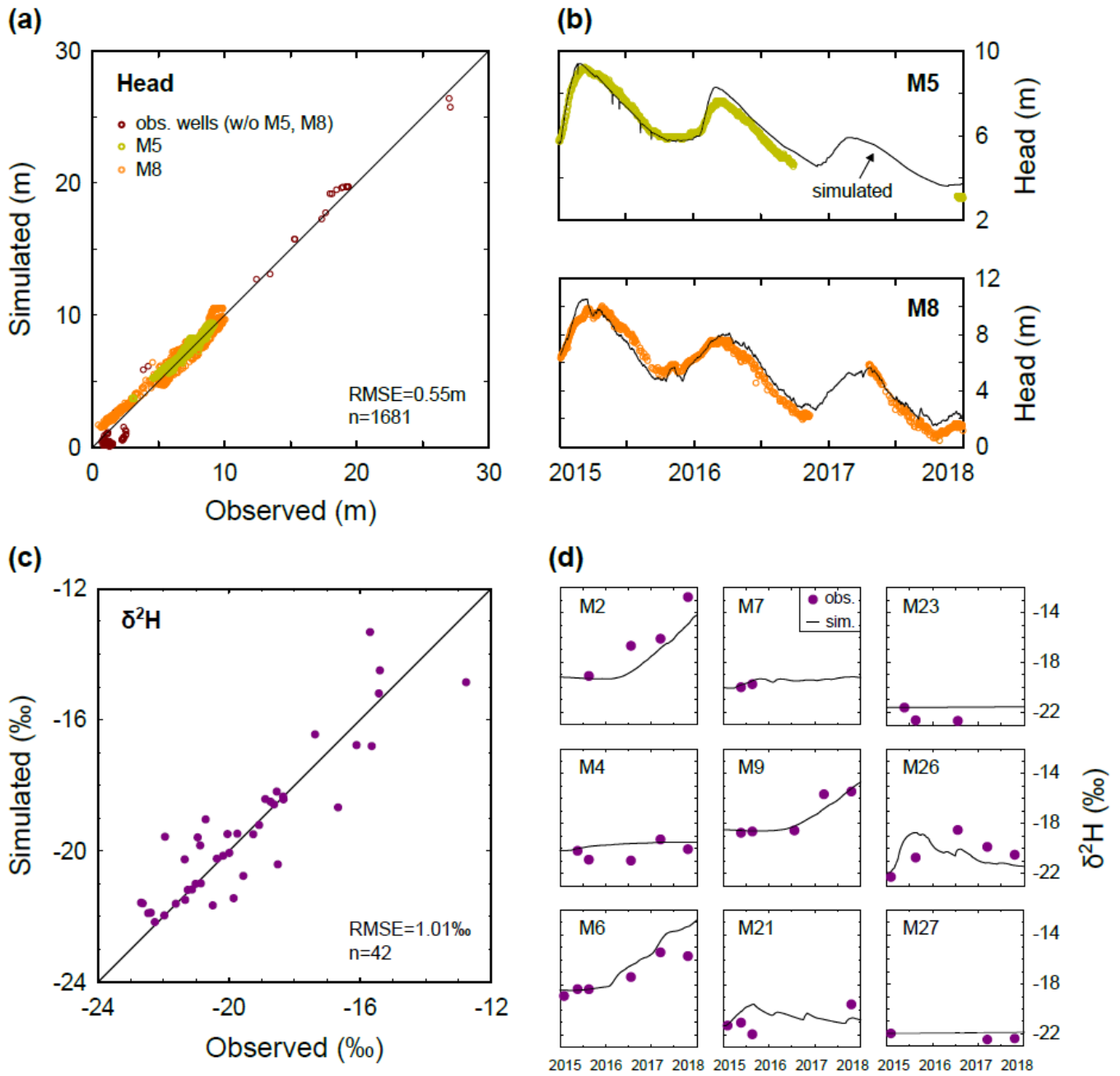
166 **Figure 3. (a) Water isotopic composition of the production wells (GW) and reverse-osmosis desalinated seawater (DSW); the eastern**  
 167 **Mediterranean meteoric water line (EMMWL) is shown for comparison (Gat and Dansgaard, 1972). (b) Chloride ( $\text{Cl}^-$ ) and  $\delta^2\text{H}$**   
 168 **sampled in nine production wells at the Menashe MAR site.**

### 169 3.2 Model

#### 170 3.2.1 Calibration

171 The flow model was calibrated against head data from 13 wells (Fig. 4a). We used mainly continuous head data measured at  
 172 two production wells, M5 and M8 (Fig. 4b). Well M5, situated 400 m SE of pond 3 and exploiting aquifer layers bounded  
 173 between -16 to -54 m MSL, was inactive during 2015-7, making it ideal for head monitoring. Well M8, situated 1 km north of  
 174 pond 3 and exploiting aquifer layers bounded between -14 to -48 m MSL, was used for production during some of the study  
 175 period, and thus only selected head data (representing quasi-static heads) were used for calibration.

176 The transport model was calibrated against isotope data from 12 wells (M2-4, M6-10, M21, M23, and M26-27; Fig. 4c).  
 177 Specifically, we used data corresponding to the breakthrough of DSW in the down-gradient (western) production wells near  
 178 the DSW infiltration pond (M2, M6, and M9), since other wells showed smaller  $\delta^2\text{H}$  variations (Fig. 4d). The simulated  
 179 groundwater heads and  $\delta^2\text{H}$  for the calibration period are generally in good agreement with observations. The calibrated  
 180 hydrological parameters are specified in Table 2.



181  
 182  
 183  
 184

**Figure 4. Model calibration. (a) Comparison of simulated and observed hydraulic head. (b) Temporal variations of simulated and observed hydraulic head in wells M5 and M8. (c) Comparison of simulated and observed  $\delta^2\text{H}$ . (d) Temporal variations of simulated and observed  $\delta^2\text{H}$  in nine selected wells.**

185 **Table 2. Calibrated parameters used for the different hydro-geological units.**

Hydro-geological unit	1	2	3	4
Horizontal K (m d <sup>-1</sup> )	50	12	6	0.01
Vertical K (m d <sup>-1</sup> )	12.5	3	1.5	0.01
Specific storage (m <sup>-1</sup> )	0.002	0.0015	0.001	0.001
Specific yield	0.35	0.12	0.12	0.1
Longitudinal dispersivity <sup>a</sup> (m)	20	20	20	20
Porosity	0.35	0.19	0.17	0.1

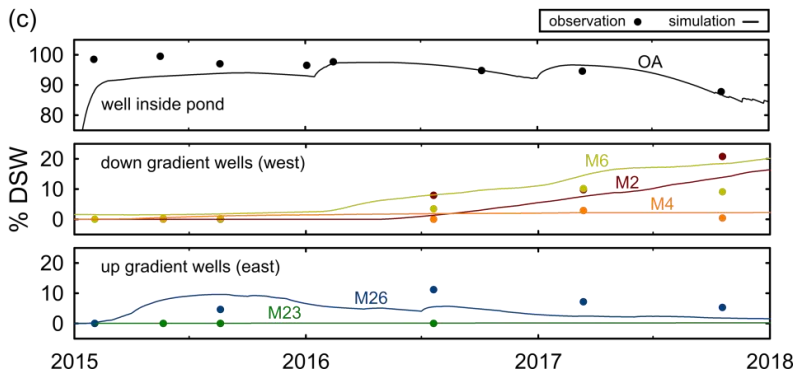
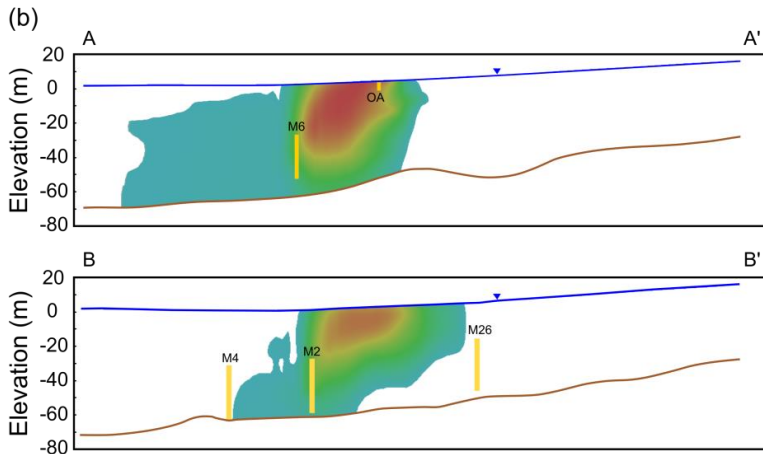
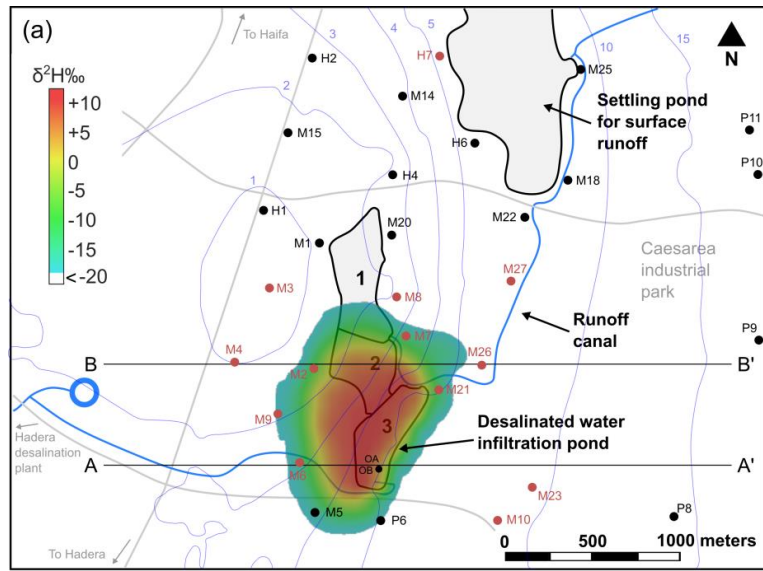
186 <sup>a</sup>Transverse horizontal and vertical dispersivities are 0.1 and 0.01, respectively, of the longitudinal dispersivity (Burnett and Frind, 1987).  
 187

### 188 3.2.2 DSW spreading in the aquifer

189 Our simulations show that at the end of 2017 the DSW plume is spreading westwards (in the direction of the natural hydraulic  
 190 gradient, as expected), approaching the closest western production wells (M2, M6, M9; Fig. 5a). Note that the production wells  
 191 to the east (up-gradient) show constant  $\delta^2\text{H}$ , indicating no interaction with the DSW recharge. Variability of  $\delta^2\text{H}$  along the  
 192 production wells screens (in the vertical direction), implies that the measured  $\delta^2\text{H}$  is a mixture of several aquifer layers (Fig.  
 193 5b).

194 The  $\delta^2\text{H}$  variations shown in Fig. 5a reflect the DSW spreading in the aquifer. The highest  $\delta^2\text{H}$  that was measured in the aquifer  
 195 (prior to MAR of DSW) was  $\delta^2\text{H}=18.41\text{‰}$  and therefore any value above it indicates mixing with DSW. However, because  
 196 the initial measured  $\delta^2\text{H}$  values in the aquifer are in the range of  $\delta^2\text{H}=-18.41\text{‰}$  to  $-22.68\text{‰}$ , the extent of DSW mixing in each  
 197 well is relative to its specific initial  $\delta^2\text{H}$ . This can be calculated by a mixing ratio (MR) approach with  $\text{MR}=(\delta_w - \delta_i)/(\delta_{\text{DSW}} -$   
 198  $\delta_i)$ , where  $\delta_w$  is the  $\delta^2\text{H}$  in the well,  $\delta_i$  is the initial (background)  $\delta^2\text{H}$  in the well and  $\delta_{\text{DSW}}$  is the  $\delta^2\text{H}$  of DSW. The MR value  
 199 of 0 and 1, implies original aquifer water and pure DSW, respectively. Fig. 5c shows the MR (expressed in %DSW) of three  
 200 down-gradient wells (M2, M4 and M6), two up-gradient well (M23 and M26) and an observation well (OA) inside the DSW  
 201 pond. Wells M2 and M6 have up to 20% DSW portion while M23 and OA retain original aquifer water and almost pure DSW,  
 202 respectively. At the end of 2017, about 7% of the recharged DSW was recovered by the production wells.

203 Knowing the water composition of the aquifer and of DSW, and assuming a conservative transport of all the major ions, one  
 204 can estimate the water composition in a specific well based on the calculated mixing ratio,  $[X]_w=\text{MR}\times[X]_{\text{DSW}}+(1-\text{MR})\times[X]_i$ .  
 205 Here  $[X]_w$  is the (calculated) ion concentration in the well,  $[X]_{\text{DSW}}$  is the ion concentration in the DSW, and  $[X]_i$  is the initial  
 206 ion concentration (background) in the well. Diversion of the observed concentration from the calculated concentration can  
 207 give insight to the sediment-water reaction (e.g., Ganot et al., 2018; Ronen-Eliraz et al., 2017; Stuyfzand et al., 2017).



208

209

210

211

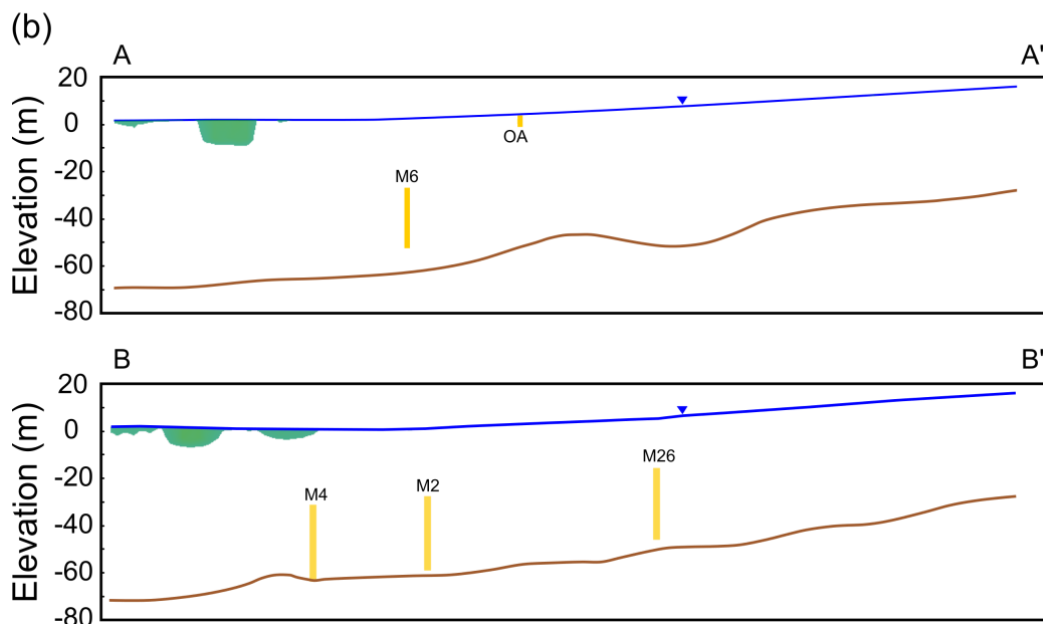
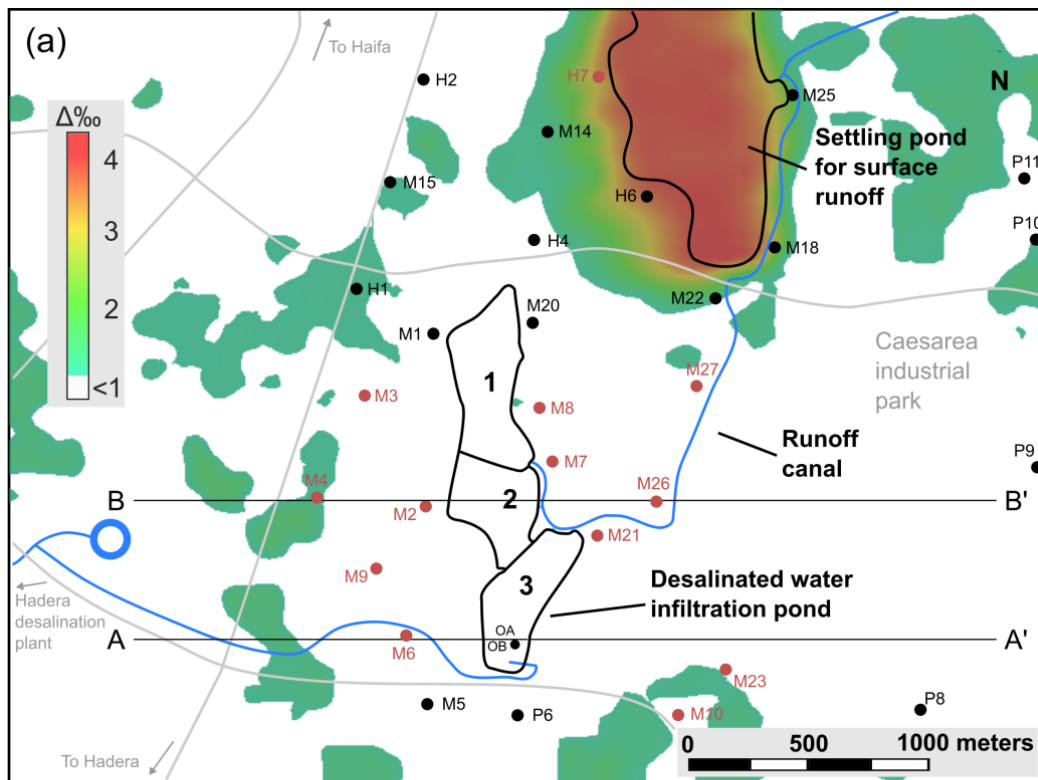
212

**Figure 5.** Simulation results showing DS2H spreading at the end of 2017. (a) Plan view (water blue); colored area shows the DS2H plume, white area indicates natural GW ( $\delta^2\text{H} < -20\text{‰}$ ) and blue contours are GW head. (b) Cross-sections east-west through wells OA and M6 (A-A') and wells M4, M2 and M26 (B-B'); well screens are shown in yellow. (c) Observed and simulated DS2H fraction (%) in selected wells along the cross-sections A-A' and B-B'.

### 213 3.2.3 Binary system assumption

214 The model was based on the assumption that all water types in this system can be described by two end-members sorted by  
215 their isotope composition: (1) the ‘heavy’ DSW ( $\delta^2\text{H}=11.34\text{‰}$ ); and (2) the ‘light’ natural water ( $\delta^2\text{H}=-22.68\text{‰}$ ) which  
216 includes all other water types (rain, runoff and GW). As pointed out before, while DSW isotope composition is constant, that  
217 of the local natural water is more variable. To examine the validity of the assumption of binary  $\delta^2\text{H}$  values, we ran the  
218 simulation again for the same period of 2015 to 2017, but this time with the maximum value of GW  $\delta^2\text{H}=-18.41\text{‰}$  (in all GW  
219 boundaries and also as rain and runoff source) in order to check the model sensitivity to the natural GW isotope variability.  
220 We subtracted the isotope composition results of the two simulations in all model cells to produce an error map (Fig. 6a) of  
221  $\delta^2\text{H}$  differences ( $\Delta\text{‰}$ ). In terms of  $\delta^2\text{H}$  composition in the production wells (Fig. 6b), the results of both simulations were  
222 similar ( $\Delta\text{‰}<1$ ), while some differences (up to  $\Delta\text{‰}=4.3$ ) were found in the domain boundaries and at the upper layer that was  
223 affected by rain and runoff recharge. Specifically, a notable difference is seen in the runoff settling pond which is a source of  
224 natural water recharge. Nevertheless, for the area surrounding the DSW infiltration basin (pond 3), the binary assumption is  
225 valid due to the following conditions: (1) the distinct difference between the isotope composition of DSW and GW; (2) the  
226 model boundaries are relatively far ( $>2$  km) from the source of MAR with DSW; and (3) the screens of the production wells  
227 are relatively deep (depth  $>50$  m). Hence, in this case we can conclude that the initial variability of isotope composition in the  
228 aquifer has a negligible impact on the simulation results. Practically, it implies that interpolation efforts of the aquifer isotope  
229 composition (prior to MAR with DSW) are unnecessary as one can use an average isotope value to normalize the tracer  
230 concentration in the aquifer. In addition, A major advantage of ~~this the~~ binary assumption is that it allows to estimate mixing  
231 when the spatial data of water isotope is limited. This was exploited in the current study, where isotope data of the model  
232 boundaries was unavailable.

233 The results of the error analysis also support the model assumption that isotope fractionation is negligible during GW flow  
234 (i.e., isotope composition is conservative) as the isotope composition variability in the aquifer (which originate from  
235 fractionation processes) does not impact the simulation results (Fig. 6). Moreover, our measurements at the Menashe MAR  
236 site show similar isotope composition between the DSW source-water at the surface, in the variably-saturated zone and at the  
237 shallow GW (Ganot et al., 2018). Therefore, even if isotope fractionation exists in the aquifer to some extent as a slow process,  
238 it should be considered negligible compared to the distinct difference between the isotope end-members.

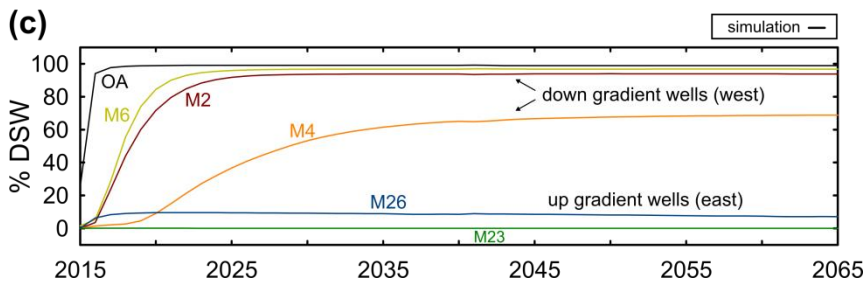
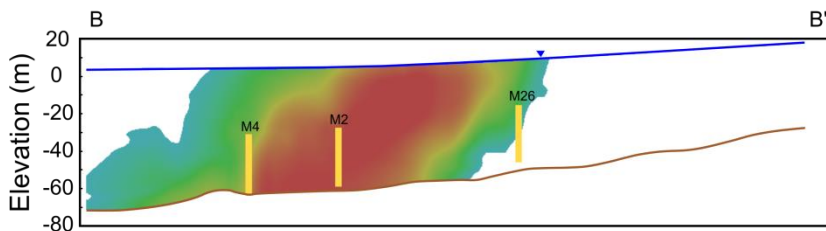
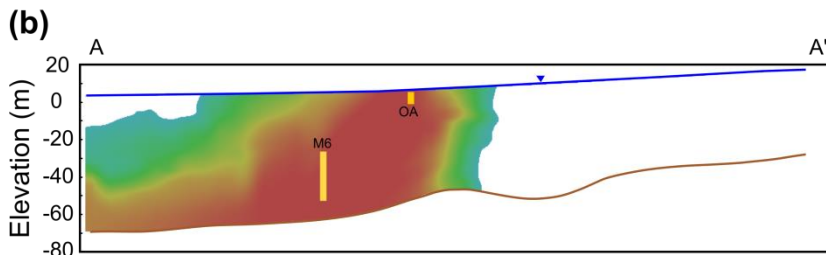
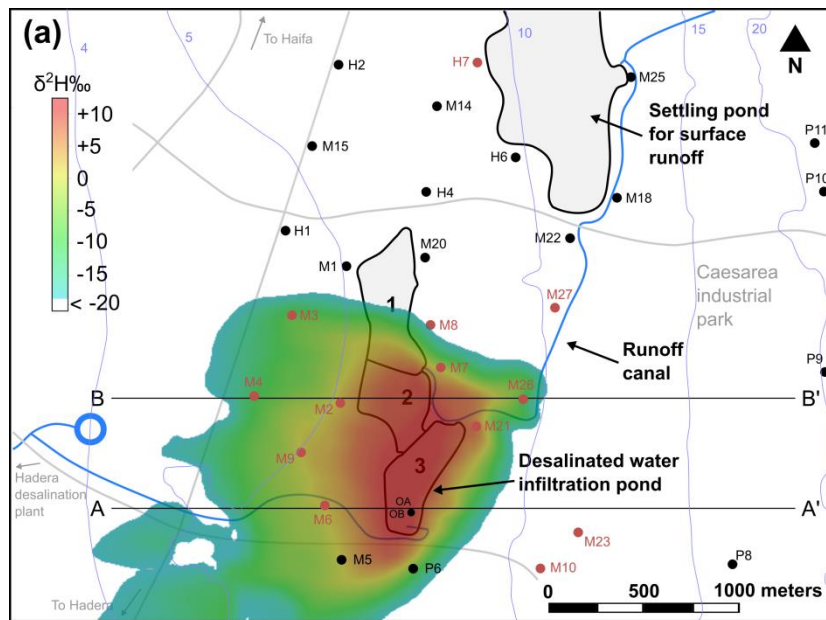


239

240 **Figure 6. Examination of the validity of the assumption of binary isotopic mixing.** (a) Plan view (water table) of  $\delta^2\text{H}$  difference ( $\Delta\text{‰}$ )  
 241 between simulation results (2015-2017) with  $\delta^2\text{H}_{\text{max}}=-18.41\text{‰}$  ( $C_{\text{GW}}=0.13$ ) and  $\delta^2\text{H}_{\text{min}}=-22.68\text{‰}$  ( $C_{\text{GW}}=0$ ) at the end of 2017; white  
 242 area indicates  $\Delta\text{‰}<1$ . (b) Cross-sections east-west through wells OA and M6 (A-A') and wells M4, M2 and M26 (B-B'); well screens  
 243 are shown in yellow.

#### 244 3.2.4 Predicting long-term DSW spreading in the aquifer (2015-2065)

245 We test the extent of DSW spreading in the aquifer by performing long-term (50 years) simulation of MAR with DSW,  
246 considering 50 repeated annual cycles of the hydraulic conditions recorded in 2015, with a MAR event of 2.6 MCM (Fig. 7a).  
247 ~~As expected~~ According to the simulation results, the water in the down-gradient (westwards) wells closest to the DSW pond,  
248 M2 and M6, ~~are~~ will be fully exchanged by DSW after 10 years of MAR, while the up-gradient wells show little (M26) or no  
249 mixing (M23) with DSW (Fig. 7b,c). Interestingly, well M4 located further to the west, reaches a steady DSW mixing of  
250 almost 70% after about 35 years of MAR without being fully exchanged by DSW, while the DSW plume continues to progress  
251 further west. By the end of 2065, the total DSW volume of 130 MCM recharged at the infiltration pond ~~is~~ will be distributed  
252 as follows: 114 MCM (88%) is recovered by the western pumping wells (M2-9, P6), 8.4 MCM (6%) by the eastern pumping  
253 wells (M21, M26), with only 7.5 MCM (6%) remaining in the aquifer.



254

255

256

257

258

**Figure 7.** Long-term simulations of DSW spreading at the end of 2065 after 50 years of MAR. (a) Plan view (water table); colored area shows the DSW plume, white area indicates natural GW ( $\delta^2\text{H} < -20\text{‰}$ ) and blue contours are GW head. (b) Cross-sections east-west through wells OA and M6 (A-A') and wells M4, M2 and M26 (B-B'); well screens are shown in yellow. (c) Simulated DSW fraction (%) in selected wells along the cross-sections A-A' and B-B'.

#### 259 4. Conclusions

260 We track the fate of reverse-osmosis DSW that were introduced to groundwater by MAR, using stable water isotopes. The use  
261 of the water isotopes of  $^{18}\text{O}$  and  $^2\text{H}$  is advantageous in this system for two reasons: (1) there is a distinct difference between  
262 the isotope composition of DSW and natural fresh water; and (2) the water isotope composition of all natural water sources—  
263 groundwater-(GW), rain and runoff—is very similar. The former makes water stable isotopes a more sensitive tracer (compared  
264 to other natural conservative tracers such as chloride), whereas the latter reduces the problem to a binary mixture of two end-  
265 members: reverse-osmosis DSW and natural GW. We formulate a detailed three-dimensional GW flow and transport model,  
266 exploiting these advantages. The model, calibrated using field data (measured during 2015-2017), is used to predict the  
267 spreading of DSW in the aquifer during 50 years of MAR with DSW. Our simulation results ~~show~~-suggest that most of the  
268 recharged DSW (94%) is recovered by the production wells, indicating the efficacy of the Menashe MAR site. ~~The presented  
269 methodology is valuable for predicting DSW plume spreading in natural groundwater aquifers.~~  
270 The advantage of using stable water isotopes for tracing reverse-osmosis DSW in various downstream water systems is already  
271 known from previous studies. In this study we used this advantage in a modeling framework to predict future mixing and  
272 spreading trends of DSW in ~~the~~an aquifer. Hence, this modeling approach can be used in other MAR sites (e.g., Mazariegos  
273 et al., 2017; Negev et al., 2017; Stuyfzand et al., 2017) to predict reverse-osmosis DSW distribution in aquifers. As the  
274 production of DSW using reverse-osmosis is projected to increase and the use of MAR systems expands, we believe that the  
275 methodology presented in this paper will be highly relevant for more MAR hydrologists.

#### 276 Acknowledgments

277 The research leading to these results received funding from the Germany-Israel binational scientific cooperation BMBF-  
278 MOST, Project WT1401. We thank Amos Russak and Raz Studny (Ben-Gurion University) for sampling and analysis  
279 assistance.

#### 280 References

- 281 Al-Basheer, W., Al-Jalal, A. and Gasmi, K.: Variations in isotopic composition of desalinated water, *Water and Environment*  
282 *Journal*, 31(2), 209–214, doi:10.1111/wej.12232, 2017.
- 283 Birnhack, L., Voutchkov, N. and Lahav, O.: Fundamental chemistry and engineering aspects of post-treatment processes for  
284 desalinated water—A review, *Desalination*, 273(1), 6–22, doi:10.1016/j.desal.2010.11.011, 2011.
- 285 Boronina, A., Balderer, W., Renard, P. and Stichler, W.: Study of stable isotopes in the Kouris catchment (Cyprus) for the  
286 description of the regional groundwater flow, *Journal of Hydrology*, 308(1), 214–226, doi:10.1016/j.jhydrol.2004.11.001,  
287 2005.

- 288 Burnett R. D. and Frind E. O.: Simulation of contaminant transport in three dimensions: 2. Dimensionality effects, *Water*  
289 *Resources Research*, 23(4), 695–705, doi:10.1029/WR023i004p00695, 1987.
- 290 Carle, S. F.: T-PROGS: Transition probability geostatistical software, University of California, Davis, CA, 84 [online]  
291 Available from: <http://gmsdocs.aquaveo.com/t-progs.pdf> (Accessed 15 August 2017), 1999.
- 292 Dawoud, M. A.: The role of desalination in augmentation of water supply in GCC countries, *Desalination*, 186(1–3), 187–  
293 198, doi:10.1016/j.desal.2005.03.094, 2005.
- 294 Dreizin, Y., Tenne, A. and Hoffman, D.: Integrating large scale seawater desalination plants within Israel’s water supply  
295 system, *Desalination*, 220(1–3), 132–149, doi:10.1016/j.desal.2007.01.028, 2008.
- 296 Ganot, Y., Holtzman, R., Weisbrod, N., Nitzan, I., Katz, Y. and Kurtzman, D.: Monitoring and modeling infiltration–  
297 recharge dynamics of managed aquifer recharge with desalinated seawater, *Hydrol. Earth Syst. Sci.*, 21(9), 4479–4493,  
298 doi:10.5194/hess-21-4479-2017, 2017.
- 299 Ganot, Y., Holtzman, R., Weisbrod, N., Russak, A., Katz, Y. and Kurtzman, D.: Geochemical Processes During Managed  
300 Aquifer Recharge With Desalinated Seawater, *Water Resources Research*, 54(2), 978–994, doi:10.1002/2017WR021798,  
301 2018.
- 302 Gat, J. R.: Oxygen and hydrogen isotopes in the hydrologic cycle, *Annual Review of Earth and Planetary Sciences*, 24(1),  
303 225–262, 1996.
- 304 Gat, J. R. and Dansgaard, W.: Stable isotope survey of the fresh water occurrences in Israel and the Northern Jordan Rift  
305 Valley, *Journal of Hydrology*, 16(3), 177–211, doi:10.1016/0022-1694(72)90052-2, 1972.
- 306 Goldsmith, Y., Polissar, P. J., Ayalon, A., Bar-Matthews, M., deMenocal, P. B. and Broecker, W. S.: The modern and Last  
307 Glacial Maximum hydrological cycles of the Eastern Mediterranean and the Levant from a water isotope perspective, *Earth*  
308 *and Planetary Science Letters*, 457, 302–312, doi:10.1016/j.epsl.2016.10.017, 2017.
- 309 Gvirtzman, H.: Israel Water Resources, Chapters in Hydrology and Environmental Sciences, Yad Ben-Zvi Press, Jerusalem.,  
310 2002.
- 311 Hanasaki, N., Yoshikawa, S., Kakinuma, K. and Kanae, S.: A seawater desalination scheme for global hydrological models,  
312 *Hydrol. Earth Syst. Sci.*, 20(10), 4143–4157, doi:10.5194/hess-20-4143-2016, 2016.
- 313 Harbaugh, A. W., Banta, E. R., Hill, M. C. and McDonald, M. G.: MODFLOW-2000, The U.S. Geological Survey Modular  
314 Ground-Water Model - User Guide to Modularization Concepts and the Ground-Water Flow Process, Report. [online]  
315 Available from: <http://pubs.er.usgs.gov/publication/ofr200092>, 2000.
- 316 Israel Meteorological Service, <http://www.ims.gov.il/IMS/CLIMATE/ClimaticAtlas/> (Accessed 4 June 2018), 2014.
- 317 Israel Water Authority, [http://www.water.gov.il/Hebrew/ProfessionalInfoAndData/Data-](http://www.water.gov.il/Hebrew/ProfessionalInfoAndData/Data-Hidrologeime/DocLib2/hydrological-report-sep14.pdf)  
318 [Hidrologeime/DocLib2/hydrological-report-sep14.pdf](http://www.water.gov.il/Hebrew/ProfessionalInfoAndData/Data-Hidrologeime/DocLib2/hydrological-report-sep14.pdf) (Accessed 4 June 2018), 2014.
- 319 Israel Water Authority, [http://www.water.gov.il/Hebrew/ProfessionalInfoAndData/Allocation-Consumption-and-](http://www.water.gov.il/Hebrew/ProfessionalInfoAndData/Allocation-Consumption-and-production/20173/intro.pdf)  
320 [production/20173/intro.pdf](http://www.water.gov.il/Hebrew/ProfessionalInfoAndData/Allocation-Consumption-and-production/20173/intro.pdf) ~~[http://www.water.gov.il/Hebrew/ProfessionalInfoAndData/Allocation-Consumption-and-](http://www.water.gov.il/Hebrew/ProfessionalInfoAndData/Allocation-Consumption-and-production/20171/summary.pdf)~~  
321 ~~[production/20171/summary.pdf](http://www.water.gov.il/Hebrew/ProfessionalInfoAndData/Allocation-Consumption-and-production/20171/summary.pdf)~~ (Accessed 4-19 June-November 2018), ~~2017~~2018.

- 322 Kloppmann, W., Vengosh, A., Guerrot, C., Millot, R. and Pankratov, I.: Isotope and Ion Selectivity in Reverse Osmosis  
 323 Desalination: Geochemical Tracers for Man-made Freshwater, *Environmental Science & Technology*, 42(13), 4723–4731,  
 324 doi:10.1021/es7028894, 2008a.
- 325 Kloppmann, W., Van Houtte, E., Picot, G., Vandenbohede, A., Lebbe, L., Guerrot, C., Millot, R., Gaus, I. and Wintgens, T.:  
 326 Monitoring Reverse Osmosis Treated Wastewater Recharge into a Coastal Aquifer by Environmental Isotopes (B, Li, O, H),  
 327 *Environmental Science & Technology*, 42(23), 8759–8765, doi:10.1021/es8011222, 2008b.
- 328 Kloppmann, W., Negev, I., Guttman, J., Goren, O., Gavrieli, I., Guerrot, C., Flehoc, C., Pettenati, M. and Burg, A.: Massive  
 329 arrival of desalinated seawater in a regional urban water cycle: A multi-isotope study (B, S, O, H), *Science of The Total*  
 330 *Environment*, 619–620, 272–280, doi:10.1016/j.scitotenv.2017.10.181, 2018.
- 331 Krabbenhoft, D. P., Anderson, M. P. and Bowser, C. J.: Estimating groundwater exchange with lakes: 2. Calibration of a  
 332 three-dimensional, solute transport model to a stable isotope plume, *Water Resour. Res.*, 26(10), 2455–2462,  
 333 doi:10.1029/WR026i010p02455, 1990.
- 334 Kurtzman, D., Netzer, L., Weisbrod, N., Nasser, A., Graber, E. R. and Ronen, D.: Characterization of deep aquifer dynamics  
 335 using principal component analysis of sequential multilevel data, *Hydrology and Earth System Sciences*, 16(3), 761–771,  
 336 doi:10.5194/hess-16-761-2012, 2012.
- 337 Lahav, O., Kochva, M. and Tarchitzky, J.: Potential drawbacks associated with agricultural irrigation with treated  
 338 wastewaters from desalinated water origin and possible remedies, *Water Science & Technology*, 61(10), 2451,  
 339 doi:10.2166/wst.2010.157, 2010.
- 340 Liu, Y., Yamanaka, T., Zhou, X., Tian, F. and Ma, W.: Combined use of tracer approach and numerical simulation to  
 341 estimate groundwater recharge in an alluvial aquifer system: A case study of Nasunogahara area, central Japan, *Journal of*  
 342 *Hydrology*, 519, 833–847, doi:10.1016/j.jhydrol.2014.08.017, 2014.
- 343 Mazariegos, J. G., Walker, J. C., Xu, X. and Czimczik, C. I.: Tracing Artificially Recharged Groundwater using Water and  
 344 Carbon Isotopes, *Radiocarb. Tucson*, 59(2), 407–421, doi:http://dx.doi.org/10.1017/RDC.2016.51, 2017.
- 345 Negev, I., Guttman, J. and Kloppmann, W.: The Use of Stable Water Isotopes as Tracers in Soil Aquifer Treatment (SAT)  
 346 and in Regional Water Systems, *Water*, 9(2), 73, doi:10.3390/w9020073, 2017.
- 347 Reynolds, D. A. and Marimuthu, S.: Deuterium composition and flow path analysis as additional calibration targets to  
 348 calibrate groundwater flow simulation in a coastal wetlands system, *Hydrogeol J*, 15(3), 515–535, doi:10.1007/s10040-006-  
 349 0113-5, 2007.
- 350 Rodríguez-Escales, P., Canelles, A., Sanchez-Vila, X., Folch, A., Kurtzman, D., Rossetto, R., Fernández-Escalante, E.,  
 351 Lobo-Ferreira, J.-P., Sapiano, M., San-Sebastián, J. and Schüth, C.: A risk assessment methodology to evaluate the risk  
 352 failure of managed aquifer recharge in the Mediterranean Basin, *Hydrology and Earth System Sciences*, 22(6), 3213–3227,  
 353 doi:10.5194/hess-22-3213-2018, 2018.
- 354 Ronen-Eliraz, G., Russak, A., Nitzan, I., Guttman, J. and Kurtzman, D.: Investigating geochemical aspects of managed  
 355 aquifer recharge by column experiments with alternating desalinated water and groundwater, *Science of The Total*  
 356 *Environment*, 574, 1174–1181, doi:10.1016/j.scitotenv.2016.09.075, 2017.
- 357 Sellinger, A. and Aberbach, S.: Artificial recharge of coastal-plain aquifer in Israel, *Underground Waste Management and*  
 358 *Artificial Recharge*, 2, 1973.

- 359 Shavit, U. and Furman, A.: The location of deep salinity sources in the Israeli Coastal aquifer, *Journal of Hydrology*, 250(1–  
360 4), 63–77, doi:10.1016/S0022-1694(01)00406-1, 2001.
- 361 Stanhill, G., Kurtzman, D. and Rosa, R.: Estimating desalination requirements in semi-arid climates: A Mediterranean case  
362 study, *Desalination*, 355, 118–123, doi:10.1016/j.desal.2014.10.035, 2015.
- 363 Stichler, W., Maloszewski, P., Bertleff, B. and Watzel, R.: Use of environmental isotopes to define the capture zone of a  
364 drinking water supply situated near a dredge lake, *Journal of Hydrology*, 362(3), 220–233,  
365 doi:10.1016/j.jhydrol.2008.08.024, 2008.
- 366 Stuyfzand, P. J., Smidt, E., Zuurbier, K. G., Hartog, N. and Dawoud, M. A.: Observations and Prediction of Recovered  
367 Quality of Desalinated Seawater in the Strategic ASR Project in Liwa, Abu Dhabi, *Water*, 9(3), 177, doi:10.3390/w9030177,  
368 2017.
- 369 Yermiyahu, U., Tal, A., Ben-Gal, A., Bar-Tal, A., Tarchitzky, J. and Lahav, O.: Rethinking Desalinated Water Quality and  
370 Agriculture, *Science*, 318(5852), 920–921, doi:10.1126/science.1146339, 2007.
- 371 Zheng, C. and Wang, P. P.: MT3DMS: A modular three-dimensional multi-species transport model for simulation of  
372 advection, dispersion, and chemical reactions of contaminants in ground-water systems. Documentation and user's guide, in  
373 Contract Report SERDP-99-1, U.S. Army Engineer Research and Development., 1999.
- 374 Zhou, Y. and Li, W.: A review of regional groundwater flow modeling, *Geoscience Frontiers*, 2(2), 205–214,  
375 doi:10.1016/j.gsf.2011.03.003, 2011.